

See discussions, stats, and author profiles for this publication at: <https://www.researchgate.net/publication/344595846>

Signals: From Analog to Digital, and Back (CDT-39)

Preprint · October 2020

DOI: 10.13140/RG.2.2.22748.62087/1

CITATIONS

0

READS

538

1 author:



[Luciano da F. Costa](#)

University of São Paulo

734 PUBLICATIONS 13,156 CITATIONS

[SEE PROFILE](#)

Some of the authors of this publication are also working on these related projects:



Computational Neuroscience [View project](#)



Master thesis [View project](#)

Signals: From Analog to Digital, and Back (CDT-39)

Luciano da Fontoura Costa
luciano@ifsc.usp.br

São Carlos Institute of Physics – DFCM/USP

1st Oct. 2020

Abstract

Except for phenomena taking place at the quantum level, real-world signals are almost invariably continuous along time and intensity. Yet, their respective analysis and processing by using digital computers, require three important transformations: truncating the observation of the original signal within a finite time interval, sampling along time, and discretizing the respective intensities. Inverse respective operations need to be performed when digitally modified or generated signals are to be applied to the real-world. The present work introduces and discusses the often unavoidable operations of time truncation, sampling as well as intensity quantization from the perspective of signal processing and analysis, especially with the help of frequency domain analysis as allowed by the Fourier transform, which is also briefly discussed regarding both its continuous and discrete versions. Some concepts about the electronics devices involved in analog to digital conversion, and vice-versa, are also included.

“Die Stille zwischen den Noten ist genauso wichtig wie die Noten selbst.”

W. A. Mozart

(ii) time sampling, implying the values of a signal to be sampled at each period of time; and (iii) intensity quantization, required for mapping the intensity of the signal at each sampling instant into a finite-length numeric representation.

1 Introduction

We live in a dynamic universe, where myriad events take place continuously along time and space since immemorial ages. Signals are typically associated with variations of some type of energy, such as the sound produced by wind or the light arriving from remote stars. The history of science as humanity has experienced it is inexorably related to our ability to build scientific models (e.g. [1]), which involves acquiring and analyzing signals from nature. Though most natural signals are intrinsically continuous, the advent of digital computers implied those signals to be transformed into sequences of finite length numbers that can be properly stored in finite digital memories and processed by digital circuitry. It was also thanks to these operations that so many recent scientific-technologic advancements have been obtained, including the internet.

Three main transformations are typically required for transforming an analog signal into a respective digital counterpart: (i) time truncation, in the sense that signals can only be observed along a limited interval of time;

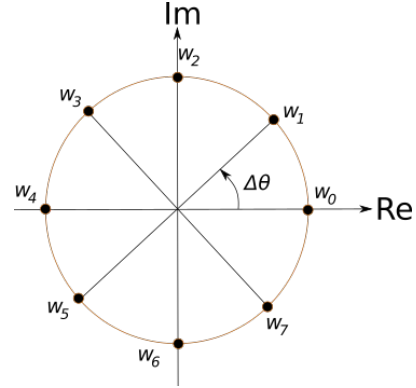


Figure 1: The complex exponential, which gives rise to the Fourier basis functions, needs to be time sampled in order to derive the discrete Fourier transform. The figure shows the distribution of w_i , $i = 0, 1, \dots, N - 1$ along the complex exponential for $N = 8$ time samples. Observe that, for simplicity's sake, positive arguments are assumed for the complex exponential.

The proper understanding of these operations is often decisive for achieving well-succeed modeling and results. The present work provides an introduction to them, with

two main highlights: extensive use of illustrations, and consideration of the transformations as characterized in the frequency domain associated to the Fourier transform, which is briefly covered in both its continuous and discrete (see Figure 1) versions. In addition, some consideration of the electronic devices typically used to implement these operations are also provided.

We start by presenting the Dirac delta and some of its properties, and follows by briefly introducing the Fourier transform, also jointly with some important respective properties. Then, the concept of convolution, as well as the associated theorem, are discussed. Having therefore covered some of the principal concepts and methods for approaching time truncation, sampling, and intensity quantization, these three important transformations are then subsequently covered and illustrated. We conclude this work by briefly discussing the basic electronic means that are typically used to interface the analog and digital worlds.

It should be observe that the present work complements another CDT, focused on the concept of convolution [2]. Other related texts that can be of interest include those addressing phase and periodicity [3], Fourier transform based edge detection [4] and curvature estimation [5]. Additional references on related topics can be found in, e.g. [6, 7, 8].

2 The Dirac Delta Function

The Dirac delta function was conceived mainly as a means for representing point discontinuities in physics, such as those implied by infinitesimal particles with mass, charge, etc. This function, traditionally represented as $\delta(t)$ has the following properties:

$$\delta(t) = \begin{cases} 0 & \text{for } t \neq 0 \\ \text{non-defined} & \text{at } t = 0 \end{cases} \quad (1)$$

Thus, the Dirac delta function assumes null values for every value of its domain variable t , except at $t = 0$, where it is not defined. As a consequence of this undefined value, the Dirac delta function is, strictly speaking, not a function. Indeed, this mathematical structure is more formally covered in the mathematical area known as *distribution theory* (e.g. [9]).

The Dirac delta can nevertheless be approached in a simple and intuitive manner, more specifically as the limit of certain types of functions. For instance, take the particular type of rectangular function defined as:

$$r(t) = \begin{cases} 0 & \text{for } t \neq 0 \\ \frac{1}{a} & \text{for } -\frac{a}{2} \leq t < \frac{a}{2} \end{cases} \quad (2)$$

where a is a positive real value. It follows immediately

that the area of the function is:

$$A = \int_{-\infty}^{\infty} r(t)dt = \int_{-\frac{a}{2}}^{\frac{a}{2}} \frac{1}{a} dt = \frac{a}{a} = 1 \quad (3)$$

The Dirac delta can now be approximated as:

$$\delta(t) = \lim_{a \rightarrow 0} r(t) \quad (4)$$

Observe that, as $a \rightarrow 0$, we have that the rectangular function becomes narrower and narrower, while its height goes higher and higher. However, given the way $r(t)$ is constructed, we necessarily have that:

$$\int_{-\infty}^{\infty} \delta(t)dt = 1 \quad (5)$$

The Dirac delta can be similarly understood as the limit of several other functions, including the normal distribution with zero means:

$$n_{\sigma} = \frac{1}{\sqrt{2\pi}\sigma} e^{-\frac{1}{2}\left(\frac{t}{\sigma}\right)^2} \quad (6)$$

More specifically, we can write:

$$\delta(t) = \lim_{\sigma \rightarrow 0} n_{\sigma}(t) \quad (7)$$

The Dirac delta can have its ‘height’ (more properly speaking, its area) generalized as:

$$a\delta(t) \quad (8)$$

where a is any real value.

It is also possible to shift the Dirac delta along time to any specific position t_0 , i.e.:

$$\delta(t - t_0) \quad (9)$$

Generally speaking, we have that:

$$\int_{-\infty}^{\infty} a\delta(t - t_0) = a \quad (10)$$

for any real values a and t_0 .

The Dirac delta provides an effective mathematical manner for representing the time sampling of signals. This involves the consideration of the so-called sampling property of the Dirac delta, expressed as:

$$\delta(t - t_0)g(t) = \delta(t - t_0)g(t_0) \quad (11)$$

Figure 2 illustrates the sampling property of the Dirac delta with respect to a generic function $g(t)$.

3 The Fourier Transform

The Fourier transform of a complex function $g(t)$ can be defined as:

$$G(f) = \int_{-\infty}^{\infty} g(t)\exp(-j2\pi ft) dt \quad (12)$$

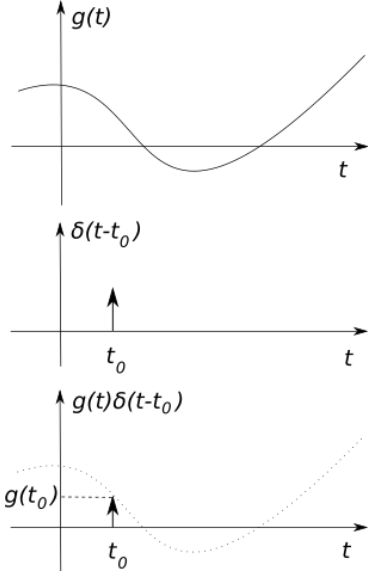


Figure 2: The sampling property of the Dirac delta. The result of multiplying a function $h(t)$ by a Dirac delta $\delta(t - t_0)$ corresponds to a Dirac delta at this same position, but with intensity $g(t_0)$.

where $j = \sqrt{-1}$.

The respective inverse Fourier transform can be expressed as:

$$g(t) = \int_{-\infty}^{\infty} G(f) \exp(j2\pi ft) df \quad (13)$$

When both $g(t)$ and $G(f)$ exist and obey Equations 12 and 13, we can write these two functions as a *Fourier transform pair*:

$$g(t) \longleftrightarrow G(f) \quad (14)$$

Observe that there are alternative manners to define the Fourier transform and its inverse, e.g. by inverting the argument of the complex exponential in both the direct and inverse transforms.

The Fourier transform of a Dirac delta can be calculated by using its sampling property as:

$$\begin{aligned} G(f) &= \int_{-\infty}^{\infty} \delta(t) \exp(-j2\pi ft) dt = \\ &= \int_{-\infty}^{\infty} \delta(t) \exp(-j2\pi f0) dt = \\ &= \int_{-\infty}^{\infty} \delta(t) \exp(0) dt = \\ &= \int_{-\infty}^{\infty} \delta(t) dt = 1 \end{aligned}$$

It can be verified that:

$$\delta(t) \longleftrightarrow 1 \quad (15)$$

The symmetry property of the Fourier transform states that:

$$G(t) \longleftrightarrow g(-f) \quad (16)$$

Applying this property on Equation 15 and observing that the Dirac delta is an even function, we derive:

$$1 \longleftrightarrow \delta(t) \quad (17)$$

Taken together, the results in Equations 15 and 17 suggest that the localization of a function in one of the domains (e.g. time or frequency) implies in the delocalization of the function at the other domain.

It can also be verified that the Fourier transform $G(f)$ of a real signal $g(t)$, which is often the case in signal processing, will have its *real part even*, i.e. $\text{Re}(G(f)) = \text{Re}(G(-f))$, and *imaginary part odd*, i.e. $\text{Im}(G(f)) = -\text{Im}(G(-f))$. This can be written more compactly as:

$$G(f) = G^*(-f) \quad (18)$$

This property ultimately derives from the symmetry of the complex exponentials constituting the basis function of the Fourier transform. Figure 3 illustrates a graphical means to interpret this fundamental property.

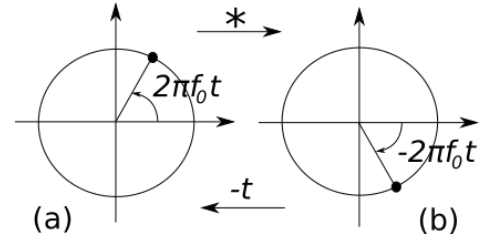


Figure 3: *Hermitian symmetry*: A complex exponential function $w(t) = \exp(j2\pi f_0 t)$ with frequency f_0 (a), and the function obtained by its conjugation (b), i.e. $w^*(t) = \exp(-j2\pi f_0 t)$. Observe that the conjugation of a complex number in the Argand plan can be geometrically interpreted as mirroring that number with respect to the real axis. It immediately follows that inverting the sense of t will recover the original function, i.e. $w^*(-t) = \exp(-j2\pi f_0(-t)) = w(t)$. In a sense, the time sign reversal acts in a way that is similar to the conjugation in the case of the complex exponential.

Another of the Fourier transform properties that is particularly useful when discussing signal sampling is the *time shifting* property, expressed as:

$$g(t - t_0) \longleftrightarrow e^{-j2\pi f t_0} G(f) \quad (19)$$

which can be verified by substituting $g(t - t_0)$ into Equation 12 and applying the variable transformation $u = t - t_0$.

Let's now consider the interesting function consisting of an infinite sum of Dirac deltas placed at $\dots, -2\Delta t, -\Delta t, 0, \Delta t, 2\Delta t \dots$, sometimes called *Dirac comb* or *shah*:

$$c_{\Delta t}(t) = \sum_{i=-\infty}^{\infty} \delta(t - i\Delta t) \quad (20)$$

By taking into account the linearity of the Fourier transform, as well as its time shifting property, we can now write:

$$C_{\Delta t}(f) = \sum_{i=\dots, -1, 0, 1, \dots} e^{-j2\pi f i \Delta t} \quad (21)$$

It can be shown, by using the Fourier series of $c_{\Delta t}(t)$ (which is periodic with period Δt), that:

$$\sum_{i=-\infty}^{\infty} \delta(t - i\Delta t) \longleftrightarrow \frac{1}{\Delta t} \sum_{i=-\infty}^{\infty} \delta\left(t - i\frac{1}{\Delta t}\right) \quad (22)$$

Figure 5 (middle line) illustrates the Dirac comb and its respective Fourier transform.

4 Convolution

The *convolution* between two complex functions $g(t)$ and $h(t)$ can be written as:

$$g(t) * h(t)[\tau] = \int_{-\infty}^{\infty} g(t)h(\tau - t)dt \quad (23)$$

This operation can be conceptually understood as a *blending* or *matching* between the two involved functions [2]. Observe that the convolution is a commutative operation.

It is interesting to consider the convolution between a function $g(t)$ and the Dirac delta $\delta(t - t_0)$:

$$\begin{aligned} g(t) * \delta(t - t_0)[\tau] &= \int_{-\infty}^{\infty} \delta(t - t_0)g(\tau - t)dt = \\ &= \int_{-\infty}^{\infty} \delta(t - t_0)g(\tau - t_0)dt = \\ &= g(\tau - t_0) \int_{-\infty}^{\infty} \delta(t - t_0)dt = \\ &= g(\tau - t_0) \end{aligned}$$

Taking into account the linearity of the Fourier transform, we can also conclude that convolving a function $g(t)$ with a Dirac comb can be understood as adding the function $g(t)$ at each position specified by one of the Dirac deltas in the respective comb.

Another result that will be especially useful for us is the *convolution theorem*, which states that:

$$\begin{aligned} g(t) * h(t) &\longleftrightarrow G(f)H(f) \\ g(t)h(t) &\longleftrightarrow G(f) * H(f) \end{aligned} \quad (24)$$

where $g(t)$ and $h(t)$ are two complex functions with respective Fourier pairs $G(f)$ and $H(f)$.

5 Signal Truncation

The observation of a real-world signal is necessarily constrained to an interval of time, which is implied both because of practical constraints (no experiment can take forever) and limited computational resources (the recording of a signal demands memory). Therefore, any real-world signal needs to be truncated (or windowed) along time.

This operation is illustrated in Figure 4, where a cosine function $x(t)$ has its duration truncated by multiplying it by a rectangular window $w(t)$. The net effect of this product is the convolution of the Fourier transforms of $x(t)$ and $w(t)$, therefore implying the Fourier transform of $x(t)$ to incorporate an unwanted oscillation caused by the blending of the original signal with the Fourier transform of the windowing function.

Observe that this effect can be ameliorated by considering wider window functions, therefore implying longer signal observation periods and larger computer memory capability for respective storage. Another interesting possibility is to consider other types of windows (e.g. [6, 7])

6 Signal Sampling

We are now in position to approach the interesting and important issue of sampling continuous signals at specific time instants. The first point to be kept in mind is that this sampling can take place at equally spaced intervals Δt , or varying intervals. For simplicity's sake, we shall be limited to the former possibility.

Figure 5 depicts a signal $g(t)$ being sampled at each Δt intervals. This can be mathematically modeled by using the Dirac delta and its sampling property. More specifically, we multiply the signal $g(t)$ (a) by the Dirac comb $C(t)$ with Δt (c), yielding the time sampled signal $g(t)C(t)$ (e). By using the convolution theorem, we obtain that this operation can be understood as the convolution between the Fourier transform of $g(t)$ (b) and the Fourier transform of $C(t)$ (d), yielding the result shown in (f). Observe that this signal is obtained by adding the Fourier transform of $g(t)$, namely $G(f)$, at each of the positions occupied by the Dirac deltas in the Fourier transform of the Dirac comb.

It is important to observe the superimposition that can occur as a consequence of the interference between subsequent adjacent sides of the Fourier transform $G(f)$. This superimposition is often called *aliasing*, effectively meaning that the maximum frequency as representable in the specific discrete Fourier domain has been exceeded. Observe that the aliasing can be reduced or even eliminated by adopting a smaller Δt . For such reasons, it is important to consider the sampling theorem, presented in the

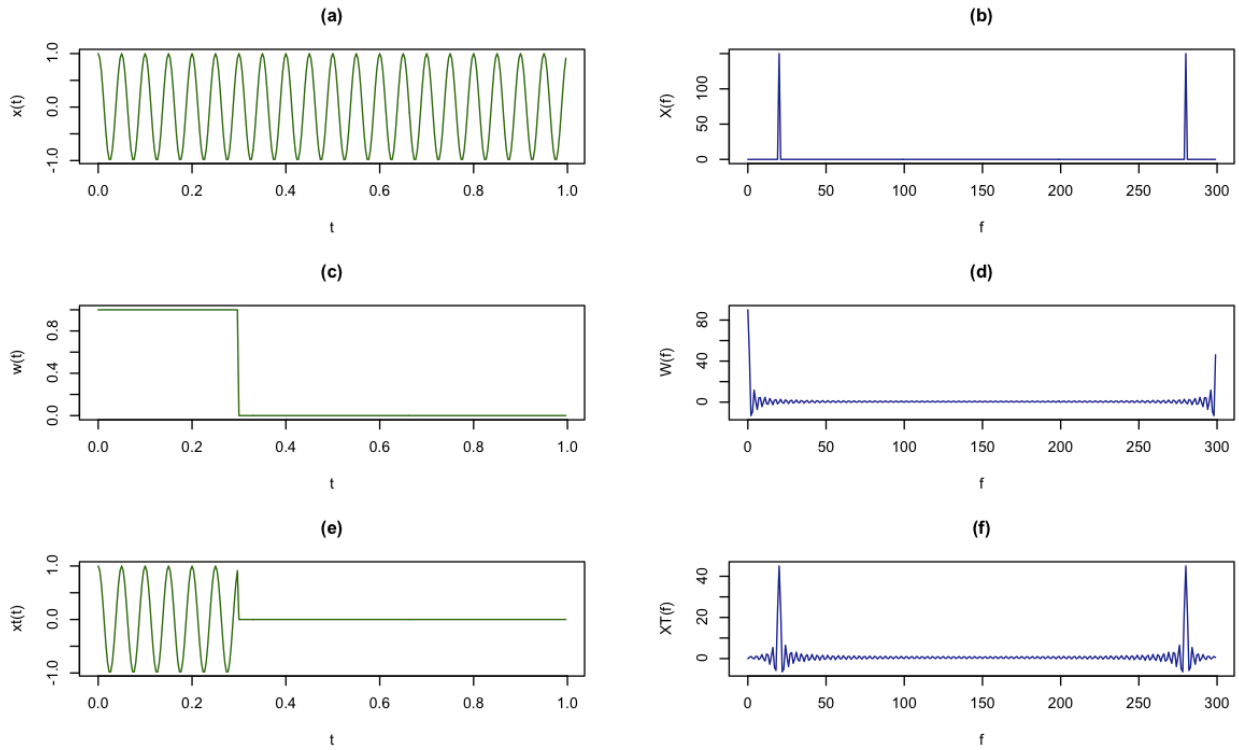


Figure 4: A cosine signal $x(t)$ fitting perfectly within the time range (a), therefore yielding a pair of sharp respective Dirac deltas in the frequency domain (b). The limitation of the observations of $x(t)$, which can be mathematically modeled by the point-by-point multiplication with a windowing function $w(t)$ of finite duration (c), whose Fourier transform corresponds to a modulated *sinc* function (d), yields a truncated version of $x(t)$ (e). The Fourier transform of this truncated function can be understood as the convolution of the functions in (a) and (b), yielding the blended result in (f). In summary: the truncation of a function along time typically implies in oscillations being added to the respective Fourier transform. Observe that only the real parts of the functions and transforms have been shown for simplicity's sake.

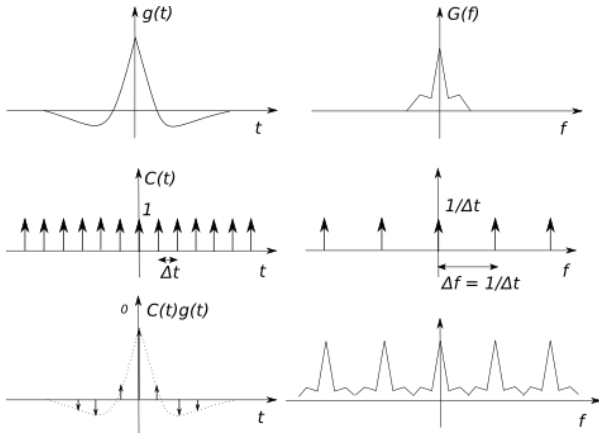


Figure 5: Time sampling a signal $g(t)$ can be mathematically modeled in terms of multiplying that respective function with a Dirac comb with resolution Δt . The resulting Fourier transform can be obtained by convolving the Fourier transform of $g(t)$ with that of the Dirac comb, yielding a periodical function with period $\Delta f = 1/\Delta t$ as result. The superimposition of the lateral portions of $G(f)$ implied by the time sampling is often known as *aliasing*, which therefore limits the maximum representable frequency.

7 The Sampling Theorem

The results developed in the previous sections allow us to approach the important problem of identifying the maximum frequency f_{max} that can be represented by a sampling procedure. This can be done immediately by observing that, as seen in the previous section, by sampling the signal with time resolution ΔT implies in obtaining a respectively periodic Fourier transform with period $\Delta f = 1/\Delta t$. Because each of these periods include both the negative and positive frequency components, we have that the maximum frequency should correspond to half the period Δf . Therefore, we can state the important sampling theorem as:

$$f_{max} = \frac{1}{2} \frac{1}{\Delta t} \quad (25)$$

8 The Discrete Fourier Transform

Considering that we almost invariably do not have an analytical description of real-world signals to be analysed, we cannot calculate their Fourier transform analytically by using continuous expressions such as that in Equa-

following section.

tion 12, which would require us to know the formula for $g(t)$. To any extent, the signals to be analysed have been time sampled along a window, which therefore yields a respective vector representation $\vec{g} = [g_i] = g(i\Delta t)$ for $i = 1, 2, \dots, N$. Thus, provided we also time sample the complex exponential $\exp(-j2\pi ft)$ in Equation 12 at the same time instants as those adopted to obtain \vec{g} , we can transform the integral of the Fourier transform into a sum, i.e.:

$$\vec{G} = G_k = \sum_{i=0,1,\dots,N-1} g_i \exp\left(-j ik \frac{2\pi}{N-1}\right) \quad (26)$$

Let's define the Fourier matrix as:

$$W = [W_{i,k}] = \exp\left(-j ik \frac{2\pi}{N-1}\right) \quad (27)$$

Observe that $\frac{2\pi}{N-1}$ effectively acts as an angular resolution $\Delta\theta$, so that we can write:

$$W = [W_{i,k}] = \exp(-j ik \Delta\theta) \quad (28)$$

For instance, in the case of $N = 8$, we have:

$$W_8 = \begin{bmatrix} \omega_0 & \omega_0 & \omega_0 & \omega_0 & \omega_0 & \omega_0 & \omega_0 & \omega_0 \\ \omega_0 & \omega_1 & \omega_2 & \omega_3 & \omega_4 & \omega_5 & \omega_6 & \omega_7 \\ \omega_0 & \omega_2 & \omega_4 & \omega_6 & \omega_0 & \omega_2 & \omega_4 & \omega_6 \\ \omega_0 & \omega_3 & \omega_6 & \omega_1 & \omega_5 & \omega_1 & \omega_4 & \omega_7 \\ \omega_0 & \omega_4 & \omega_0 & \omega_4 & \omega_0 & \omega_4 & \omega_0 & \omega_4 \\ \omega_0 & \omega_5 & \omega_2 & \omega_7 & \omega_4 & \omega_1 & \omega_6 & \omega_3 \\ \omega_0 & \omega_6 & \omega_4 & \omega_2 & \omega_0 & \omega_6 & \omega_4 & \omega_2 \\ \omega_0 & \omega_7 & \omega_6 & \omega_5 & \omega_4 & \omega_3 & \omega_2 & \omega_1 \end{bmatrix}$$

Figure 1 illustrates the distribution of the complex values ω_i along the complex exponential for $N = 8$ (we have considered positive argument of the exponential, for simplicity's sake). Observe that the initial value ω_0 is not repeated as the sampling completes the period.

The discrete Fourier transform of \vec{g} can be written as:

$$\vec{G} = W\vec{g} \quad (29)$$

This can be recognized as the general form of a *linear transformation*, which is indeed the case of the Fourier transform and many other transforms including the statistical Karhunen-Loève transform (e.g. [10]), to which the Fourier transform can be contrasted.

We also have that:

$$\vec{g} = W^{-1}\vec{G} \quad (30)$$

It can be verified that:

$$W(W^*)^T = NI \quad (31)$$

where I is the identity matrix. Observe that $(A^*)^T = (A^T)^*$ for any complex matrix A . Thus, by multiplying both sides of this equation by W^{-1} , it follows that:

$$W^{-1} = \frac{1}{N}(W^*)^T \quad (32)$$

This result indicates that the complex matrix W is *quasi-unitary*. This also means that the matrix defining the discrete inverse Fourier transform can be obtained from the direct Fourier transform matrix at low computational cost. Observe that a complex matrix A is said to be *unitary* iff its inverse is identical to its transposed conjugate. Also, the fact of a complex matrix being unitary is analogous to a real matrix being *orthogonal*.

It is interesting to observe that, whenever possible, it is often advantageous to consider calculating the discrete Fourier transform (DFT) by using some of its efficient computational implementations known as *fast Fourier transforms* — FFTs (e.g. [6, 7]). While the computational cost of the DFT with N samples is of $\mathcal{O}(N^2)$, even the simplest FFT implementation will allow a reduction to $\mathcal{O}(N \log_2 N) = \mathcal{O}(N \log N)$. Except for numerical round-off noise, the results obtained by the DFT and FFT are nearly identical.

9 Discrete Relationships

Given the extreme sensitivity of the Fourier transform in the sense that small perturbations in one domain affect generally the other domain, particular care and attention are required for indexing and representing time sampled signals and transforms.

Figure 6 illustrates the quantization of the complex exponential (a) for $N = 4$ angular or time samples, as well as the respectively implied angular (b) and time (c) representations of the real part of the sampled complex exponential, which corresponds to a cosine with *angular period* 2π and *time period* T_0 .

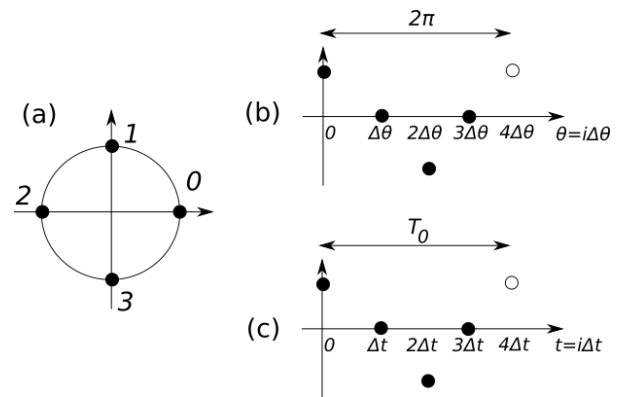


Figure 6: Relationships between the angular and time sampled complex exponential, assuming $N = 4$ samples, and respectively implied indexing and relationships. See text for explanation.

Observe that the signal quantization into N values

needs to be so that:

$$2\pi = N\Delta\theta \Rightarrow \Delta\theta = \frac{2\pi}{N} \quad (33)$$

$$T_0 = N\Delta t \Rightarrow \Delta t = \frac{T_0}{N} \quad (34)$$

Let's consider the real portion of the complex exponential with period T_0 , namely $\cos(2\pi f_0 t)$, with $f_0 = \frac{1}{T_0}$. This signal provides a good reference for better understanding the discrete indexing in the DFT, as well as the relationships between the involved variables, because it will fit exactly in the reference period T_0 .

One important point to be kept in mind is that this reference cosine with time period T_0 (and respective angular period 2π) extends from the first sample $t = 0$ up to one point before the period repetition, i.e. $(N - 1)\Delta t$, which is indicated in the fact that the last sample point in Figures 6(b) and (c) are represented as not-filled. In case the signal is allowed to go up to the next point, major unwanted oscillations will be verified in the DFT.

The first important characteristic to be noticed is that the interrelationship between the angle θ and the time t variables can be simply expressed as:

$$\frac{2\pi}{T_0} = 2\pi f_0 = \frac{\Delta\theta}{\Delta t} \quad (35)$$

Combining the above expression with Equation 34, we get:

$$f_0 = \frac{1}{T_0} = \frac{1}{N\Delta t} \quad (36)$$

which can be understood as the reference frequency associated to the reference period T_0 , with the interesting property that integer multiples of f_0 (up to the maximum representable frequency f_{max}) will be exactly sampled into the N points, therefore avoid the oscillations in the respective Fourier domain implied by the signal truncation. Actually speaking, it should be observe that it is not that these oscillations do not exist, for the time truncation is unavoidable in the DFT, but that the null-values of the oscillations in the Fourier transform of the window function coincides with the sampled values for integer multiples of the reference frequency f_0 .

We can now express the reference cosine signal, with $T_0 = 1/f_0$, as:

$$\cos(2\pi f_0 t) \approx \cos(i \Delta\theta) = \cos(2\pi f_0 i \Delta t) \quad (37)$$

where $i = 0, 1, \dots, N - 1$.

Now, the following code can be applied for setting the filter function in the respective vector with N samples, assuming $N = 100$ and $T_0 = 1$:

```
N <- 100
T0 <- 1
```

```
t <- seq(0,L,length.out=N+1)
t <- t[1:N]
dt <- t[2]
f0 <- 1/(N*dt)
x <- cos(2 * pi * f0 * t)
```

Observe the especially important instruction `t <- t[1:N]`, necessary in order to discard the repetition of the first sampled value.

10 Signal Quantization

By signal quantization we mean the round-off of the real values of a signal, as observed at each sampling step, required for obtaining a finite-length numeric representation with M bits that can be stored in a computer memory. This operation is typically performed by the electronic device known as analog to digital converter (see Section 11).

There are several ways to quantize the intensities of a signal. Figure 7 illustrates the transfer function of one of the possible schemes, with respect to 33 possible discrete levels uniformly distributed from -1 to 1 . This function is applied to each sampled value in the signal $x(t)$, yielding the sample and quantized signal $y(t)$.

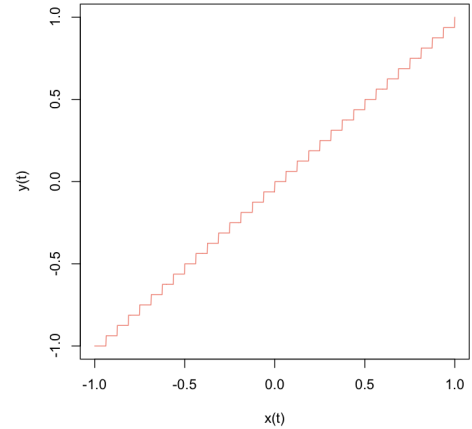


Figure 7: The transfer function of the floor quantization scheme considering 33 discrete values from -1 to 1 .

Unlike the already discussed time truncation and sampling operations, we have no simple means to mathematically model the effect of signal quantization with respect to the properties, especially in the frequency domain, of the thus obtained signals.

However, the quantization of a signal can be understood as adding high frequency (related to smaller scale details) to the original signal. As such, it is often interesting to consider low-pass filtering of quantized signals, as illustrated in Figure 12.

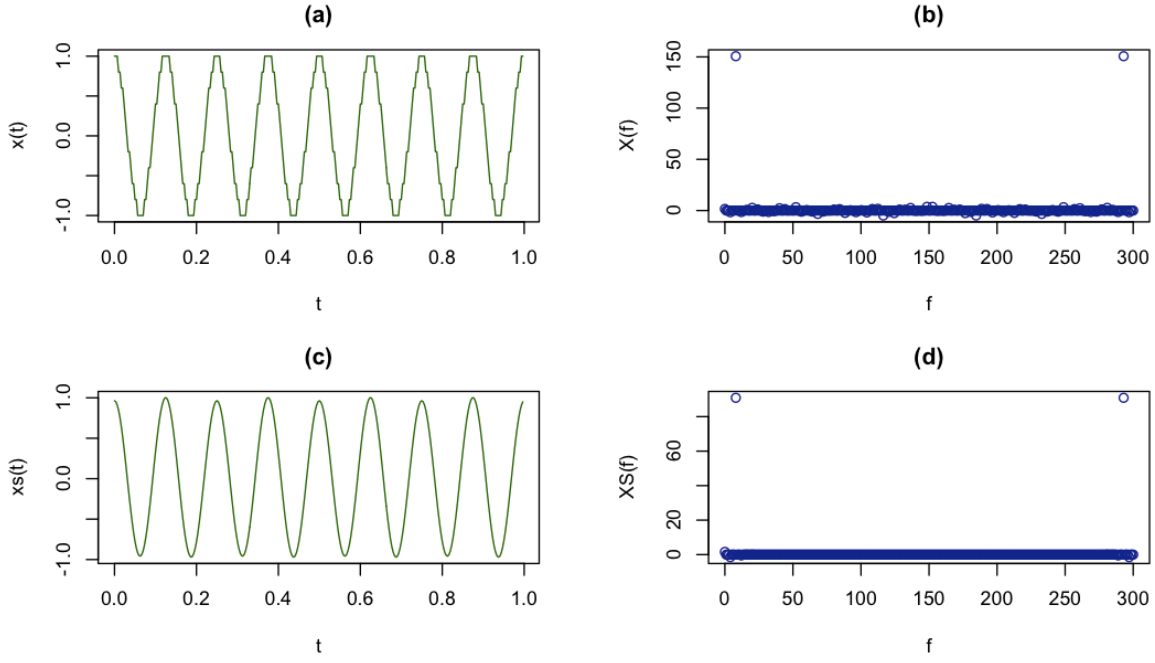


Figure 8: A cosine signal quantized using only 10 discrete levels (a), and its respective discrete Fourier transform (b), which is characterized by intense baseline noise implied by the quantization. By having the quantized signal to be smoothed by convolving it with a gaussian function, yielding (c), it is possible to reduce the high frequency quantization noise, thus achieving an improved respective Fourier transform (d). This smoothing operation can be understood in the context of regularization theory, reflecting a respective hypothesis that the signal was originally smooth. The input signal is assumed to be normalized between -1 and 1 .

The gaussian, or rather its normalized version as normal distribution (unit area), is often adopted for smoothing (low-pass filtering) a signal. Interestingly, the Fourier transform of a gaussian with standard deviation σ is also a gaussian, but with standard deviation $1/\sigma$. As such, by convolving the signal $x(t)$ with a normal function as in Equation 6, effectively we perform a low-pass filter in the frequency domain, therefore reducing the quantization effects that take place at a relatively small scale. Observe that the normal function in this operation acts as a *filter*.

Because of the periodicity of the discrete Fourier transform, special care and attention are required while setting the filter function up in the frequency domain. More specifically, the negative frequency portion of the filter function needs to be shifted to the right-hand side of the vector representing the filter function in the frequency domain, so that this function be kept coherent with the sampling of the complex exponential as traditionally considered in the discrete Fourier transform (see also [5]).

Considering a discrete Fourier transform with N sampled points, the following procedure may be considered for mounting the filter function in the frequency domain. First, we determine the two quantities NL and NR from

the number of sample N as follows:

$$NR = \text{floor}\left(\frac{N}{2}\right) \quad (38)$$

$$NL = -(N - NR - 1) \quad (39)$$

Now, the following code can be applied for setting the filter function in the respective vector with N components:

```
g <- matrix(0,1,N)
for (i in seq(0,NR))
{ g[i+1] <- exp(-0.5 *(i*dt/sig)^2) }
for (i in seq(NL,-1))
{ g[i+N+1] <- exp(-0.5 *(i*dt/sig)^2) }
```

This piece of code assumes that the vectors are indexed starting at index 1.

Figure 9 illustrates a normal function with $\sigma = 0.02$ and $N = 300$ as mounted in the respective filter vector by using the above described procedure.

Interestingly, the above described smoothing procedure acts not only on the quantization levels, but also on the sampling of the signal (especially in the case of non-uniform sampling schemes). Indeed, both these operations can be understood as implying loss of information about the original signal, and we aim at trying to recover some of the lost information. In this sense, filtering of a

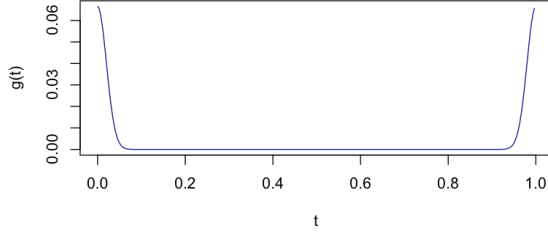


Figure 9: A normal function with $\sigma = 0.02$ and $N = 300$ as mounted into the respective filter vector by using the suggested procedure. This set-up is required so that the filter function be kept coherent, along the frequency axis, with the way in which the basis functions of the discrete Fourier transform, namely complex exponentials with successive frequencies, are traditionally sampled in implementations of that transform. Observe that the value $g(0)$ is not repeated at the end of the vector, which represents exactly one complete period in the frequency domain.

quantized signal can be understood from the perspective of the interesting research area known as *regularization theory* (e.g. [11]). In this area, hypotheses about the original signal (e.g. smoothness) are assumed in order to impose respective constraints on the incomplete signal. In our case, the main hypothesis is that the original signals are relatively smooth, so that we try to recover the respective smoothness through the low-pass filtering operation.

11 Basic Electronics of Signal Conversion

We have thus far discussed the three important transformations required for representing continuous signals predominantly from the mathematical perspective. In this section, we provide some clues about how those operations can be performed through electronic means (e.g. [12]).

Figure 10 depicts a digital to analog – DA – converter. In this type of device, the output is an analog, though limited to some possible values, signal $x(t)$ proportional to the binary input $[b_M b_{M-1} \dots b_2 b_1 b_0]$ at that time instant. As implied by their names, DA converters are intended to convert a binary value into an analog value. Observe that the resolution provided by M bits is proportional to 2^M . For instance, a DA converter with $B = 12$ bits will be capable of producing 4096 distinct values.

The counterpart of DA converter is the analog to digital converter, AD, which is illustrated in Figure 11. Here, an analog signal $x(t)$ is input, and the obtained output is a binary number proportional to the input value at each instant. Similarly to a DA converter, the resolution of an AD device is defined by the number of bits B .

Figure 12 illustrates a digital signal processing (DSP) system, including its interface with the analog environ-

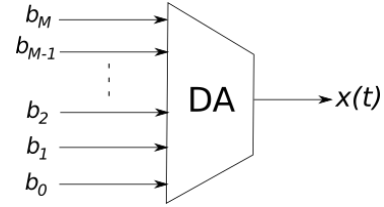


Figure 10: A typical DA converter. The output $x(t)$ is proportional to the binary value $[b_M b_{M-1} \dots b_2 b_1 b_0]$ at a given time instant.

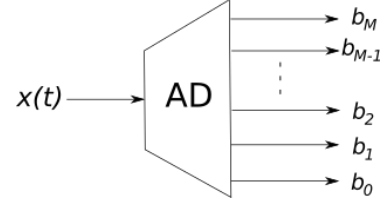


Figure 11: A typical AD converter. The input $x(t)$ is converted to a proportional binary value $[b_M b_{M-1} \dots b_2 b_1 b_0]$ at a given time instant.

ment through respective AD and DA converters. Also shown in this figure is a sample-and-hold (s/h) device, which acts as a kind of analog memory, preserving the input signal value present at each clock pulse. This device, which is sometimes incorporated into the respective AD converter, is necessary in order to keep the analog value as much constant as possible during the respective conversion.

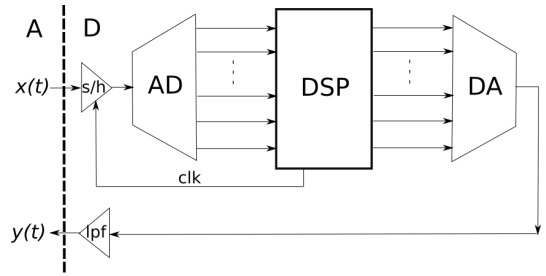


Figure 12: An overall representation of a digital signal processing system (DSP) applied to analyze the input signal $x(t)$, yielding a respective reply $y(t)$. The time sampling is performed under control of the clock (clk) signal and sample-and-hold. The signal intensity quantization if obtained through the AD converter, while the opposite operation is performed by a DA converter after the signal is processed in the DPS unit. The analog low-pass filter incorporated at the DA output is often adopted in order to reduce the quantized levels of the signals generated by the DA.

In order to reduce the high frequency noise implied by the quantized, sampled nature of the signals generated by the DA, a suitable analog low-pass filter (lpf) can be incorporated, yielding the smoother signal $y(t)$ as output (e.g. [8]).

It should be observed that systems as in Figure 12 in-

volves the integration of the two main areas of electronics, namely analog and digital circuit design.

12 Concluding Remarks

Science and technology have progressed a long way since the mechanical computers of the XIX century, redefining to a great extent the human context and experience, especially through the internet. A substantial deal of these advances and results have depended, and continue to depend, on translating signals from the analog to the digital domain, processing them in digital manner, and then deriving digital results that need to be transformed back to respective analog counterparts.

The present work aimed at providing in an introductory way the main mathematical concepts and methods for better understanding the three main transformations involved, namely: time truncation, sampling, and intensity quantization. Having introduced important concepts such as the Dirac delta sampling property, the continuous and discrete Fourier transform, as well as convolution operation and its respective theorem, we got in a position that allowed us to better understand not only the effects of signal conversion, but also to consider possible means for reducing the respective unwanted effects, such as aliasing.

There is much more to be learned regarding the interface between the analog and digital worlds (e.g. [6, 7, 8, 12]), especially regarding the analog and digital involved concepts and approaches. It is expected that the present work have motivated the reader to probe further in this interesting area.

Acknowledgments.

Luciano da F. Costa thanks CNPq (grant no. 307085/2018-0) and FAPESP (grant 15/22308-2).

References

- [1] L. da F. Costa. Modeling: The human approach to science. Researchgate, 2019. https://www.researchgate.net/publication/333389500_Modeling_The_Human_Approach_to_Science_CDT-8. [Online; accessed 1-Oct-2020].
- [2] L. da F. Costa. Convolution! Researchgate, 2019. https://www.researchgate.net/publication/336601899_Convolution_CDT-14. [Online; accessed 09-March-2020].
- [3] L. da F. Costa. Sine, cosine, periodicity, phase, sine, ... Researchgate, 2020. https://www.researchgate.net/publication/341722757_Sine_Cosine_Periodicity_Phase_Sine_CDT-33. [Online; accessed 1-Oct-2020].
- [4] L. da F. Costa. When less is more: Detecting edges in images. Researchgate, 2020. https://www.researchgate.net/publication/343862629_When_Less_is_More_Detecting_Edges_in_Images_CDT-37. [Online; accessed 1-Oct-2020].
- [5] L. da F. Costa. What can curvature tell us about shape? Researchgate, 2020. https://www.researchgate.net/publication/343651830_What_Can_Curvature_Tell_us_About_Shape_CDT-35. [Online; accessed 1-Oct-2020].
- [6] E. O. Brigham. *Fast Fourier Transform and its Applications*. Pearson, 1988.
- [7] A. V. Oppenheim and R. Schaffer. *Discrete-Time Signal Processing*. Pearson, 2009.
- [8] P. Horowitz and W. Hill. *The Art of Electronics*. Cambridge University Press, 2015.
- [9] G. van Dijk. *Distribution Theory*. De Gruyter Graduate Lectures, 2013.
- [10] F. Gewers, G. R. Ferreira, H. F. Arruda, F. N. Silva, C. H. Comin, D. R. Amancio, and L. da F. Costa. Principal component analysis: A natural approach to data exploration. Researchgate, 2019. https://www.researchgate.net/publication/324454887_Principal_Component_Analysis_A_Natural_Approach_to_Data_Exploration. accessed 1-Oct-2020.
- [11] S. Lu and S. V. Pereverzev. *Regularization Theory for Ill-posed Problems Selected Topics*. De Gruyter, 2013.
- [12] M. Pelgrom. *Analog to Digital Conversion*. Springer, 2016.

CDTs intend to be a halfway point between a formal scientific article and a dissemination text in the sense that they: (i) explain and illustrate concepts in a more informal, graphical and accessible way than the typical scientific article; and (ii) provide more in-depth mathematical developments than a more traditional dissemination work.

It is hoped that CDTs can also incorporate new insights and analogies concerning the reported concepts and methods. We hope these characteristics will contribute to making CDTs interesting both to beginners as well as to more senior researchers.

Each CDT focuses on a limited set of interrelated concepts. Though attempting to be relatively self-contained, CDTs also aim at being relatively short. Links to related material are provided in order to provide some complementation of the covered subjects.

Observe that CDTs, which come with absolutely no warranty, are non distributable and for non-commercial use only.

Please check for new versions of CDTs, as they can be revised. Also, CDTs can be cited, e.g. by including the respective DOI. The complete set of CDTs can be found at: <https://www.researchgate.net/project/Costas-Didactic-Texts-CDTs>.